Altered sterol metabolism in budding yeast affects mitochondrial iron–sulfur (Fe-S) cluster synthesis

Diane M. Ward[‡1], Opal S. Chen[§], Liangtao Li[‡], Jerry Kaplan[‡], Shah Alam Bhuiyan[¶], Selvamuthu K. Natarajan[¶], Martin Bard[¶], and James E. Cox[‖**]

From the ‡Department of Pathology, Division of Microbiology and Immunology, and the §DNA Sequencing Core, University of Utah School of Medicine, Salt Lake City, Utah 84132, the ¶Department of Biology, Indiana University-Purdue University, Indianapolis, Indiana 46202, and the ‖Department of Biochemistry and **Metabolomics Core Research Facility, University of Utah School of Medicine, Salt Lake City, Utah 84112

Edited by Joel Gottesfeld

Ergosterol synthesis is essential for cellular growth and viability of the budding yeast *Saccharomyces cerevisiae*, and intracellular sterol distribution and homeostasis are therefore highly regulated in this species. Erg25 is an iron-containing C4-methyl sterol oxidase that contributes to the conversion of 4,4-dimethylzymosterol to zymosterol, a precursor of ergosterol. The *ERG29* gene encodes an endoplasmic reticulum (ER)-associated protein, and here we identified a role for Erg29 in the methyl sterol oxidase step of ergosterol synthesis. *ERG29* deletion resulted in lethality in respiring cells, but respiration-incompetent (Rho⁻ or Rho⁰) cells survived, suggesting that Erg29 loss leads to accumulation of oxidized sterol metabolites that affect cell viability. Down-regulation of *ERG29* expression in Δ*erg29* cells indeed led to accumulation of methyl sterol metabolites, resulting in increased mitochondrial oxidants and a decreased ability of mitochondria to synthesize iron–sulfur (Fe-S) clusters due to reduced levels of Yfh1, the mammalian frataxin homolog, which is involved in mitochondrial iron metabolism. Using a high-copy genomic library, we identified suppressor genes that permitted growth of Δ*erg29* cells on respiratory substrates, and these included genes encoding the mitochondrial proteins Yfh1, Mmt1, Mmt2, and Pet20, which reversed all phenotypes associated with loss of *ERG29*. Of note, loss of Erg25 also resulted in accumulation of methyl sterol metabolites and also increased mitochondrial oxidants and degradation of Yfh1. We propose that accumulation of toxic intermediates of the methyl sterol oxidase reaction increases mitochondrial oxidants, which affect Yfh1 protein stability. These results indicate an interaction between sterols generated by ER proteins and mitochondrial iron metabolism.

Mitochondria house two iron-consuming biosynthetic pathways, heme and iron–sulfur (Fe-S)[2] cluster synthesis. In yeast, Fe-S synthesis is the essential iron-consuming process, as yeast can survive without heme or respiration but not without Fe-S cluster synthesis (1, 2). Many of the genes involved in Fe-S cluster synthesis and particularly in the mitochondrial synthesis and export of Fe-S clusters are highly conserved in all eukaryotes. Yfh1, the yeast equivalent of mammalian frataxin, plays an important role in the early steps of Fe-S cluster synthesis (3–13). Whereas the exact role has not been defined, loss of Yfh1 results in severely compromised Fe-S cluster synthesis and decreased mitochondrial function. Loss of Yfh1, as with mutations in genes in the early steps of mitochondrial Fe-S cluster synthesis, results in increased deposits of insoluble iron, "nanoparticles," within mitochondria (11). The generation of these nanoparticles results in concomitant oxidant radical formation, leading to loss of mitochondrial DNA. *YFH1* was initially identified through a genetic screen for yeast mutants that were unable to grow on low-iron medium (4). Babcock *et al.* (4) generated a mutant, *bm-8*, which was suppressed by a high-copy plasmid that contained *YFH1*. *YFH1* was acting as a high-copy suppressor and was not allelic to the mutation in *bm-8*. The *bm-8* mutant allele was a missense mutation in *YMR134W*, which encoded for a protein of unknown function. Moretti-Almeida *et al.* (14) reported that a temperature-sensitive allele of *YMR134W* showed low mitochondrial iron accumulation at the restrictive temperature along with defects in ergosterol synthesis. Here, we report a detailed description of *YMR134W*, herein referred to as *ERG29*. We determined that deletion of *ERG29* resulted in lethality in respiring cells, but cells that had lost the ability to respire (Rho⁻ or Rho⁰) could survive and that *ERG29* encodes an endoplasmic reticulum (ER) protein that plays a role in sterol synthesis at the methyl sterol oxidase step. We determined that in the absence of *ERG29*, methyl sterol metabolites accumulate and result in a decreased ability of mitochondria to synthesize Fe-S clusters. We further show that decreased Fe-S cluster synthesis is due to a dramatic reduction in Yfh1. The effects of *ERG29* loss can be exacerbated by increased mitochondrial iron import or decreased by overex-

---

[2] The abbreviations used are: Fe-S, iron–sulfur; ER, endoplasmic reticulum; 4,4-DMZ, 4,4-dimethylzymosterol; BPS, bathophenanthroline sulfonate; GE, glycerol-ethanol.

SASBMB

Table 1
Plasmids used in this study

Plasmid	Source/Reference
pGEV(Gal4:EV:VP16)	*HIS3* from Ref. 20
p*GAL1ERG29*	*TRP1* (this study)
p*GAL1ERG25*	*TRP1* (this study)
p*YCpERG29*	*URA3* (this study)
p*MET3ERG29-GFP*	*URA3* (this study)
p*YEpERG25*	*URA3* from Ref. 66
p*YEpERG26*	*URA3* from Ref. 45
p*MMT1*	*LEU2* from Ref. 25
p*MMT2*	*LEU2* from Ref. 25
p*YFH1*	*LEU2* from Ref. 5
p*MET3YFH1*	*LEU2* from Ref. 5
p*PET20*	*LEU2* (this study)
p*MET3MRS3*	*LEU2* from Ref. 25
p*MET3MMT1*	*URA3* from Ref. 25
p*MMT1/2*	*URA3* from Ref. 25

pression of mitochondrial iron exporter gene *MMT1* or *MMT2* or by overexpression of *YFH1* or *PET20*, a nuclear gene that encodes a mitochondrial protein involved in protecting mitochondria from oxidant damage (15).

Results

Deletion of ERG29 affects sterol synthesis

Erg25 is a methyl sterol oxidase, which is an essential oxo-diiron–containing enzyme located in the ER (16–18). In a complex set of reactions, Erg25 along with two other enzymes (Erg26 and Erg27) catalyzes the demethylation of 4,4-dimethylzymosterol (4,4-DMZ) to zymosterol. Preliminary studies showed that when cells with a missense mutation in *YMR134W/ERG29* were placed on low iron, they had an altered sterol pattern, similar to that seen in mutants in *ERG25* (data not shown). This finding led us to examine the effects of deletion of *ERG29*. Previous studies showed that *ERG29* was lethal in respiring cells (19). To determine the function of Erg29, we generated a *ERG29* deletion strain that contained a plasmid expressing carboxyl-terminally His-tagged Erg29 whose expression was under the control of either the β-estradiol promoter (turned on in the presence of β-estradiol, pGEV) or the *GAL1* promoter (on in the presence of galactose) (Table 1). This two-plasmid system allows for independent regulation of expression via growth in glucose with the addition of β-estradiol (no carbon source change) or via growth in galactose to permit expression and then shifted to glucose to suppress expression (20). This system also allows for tightly regulated β-estradiol–titrated expression from low to extremely high levels. Cells with a deletion in *ERG29* grown in β-estradiol were viable (Fig. 1*A*, *middle*), whereas the absence of β-estradiol resulted in a severe growth defect (Fig. 1*A*, *right*, *top left quadrant*), which over time led to the generation of small colonies. These small colonies were able to grow but were shown to be respiration-incompetent, as they were unable to grow on YPGE (Fig. 1*A*, *right*, *top right quadrant* compared with *left*, *top right quadrant*). We noted growth of Δ*erg29 p*β-estradiol-ERG29 cells on YPGE without β-estradiol (Fig. 1*A*, *left*, *top left quadrant*). As those cells were unable to grow on YPD (−) β-estradiol (Fig. 1*A*, *right*, *top left quadrant*), we attribute the growth on YPGE to the absence of glucose-mediated repression of the *GAL1* promoter in the pGEV system (20). We utilized galactose regulation of the Δ*erg29p*β-*estradiolGAL1ERG29* strain to examine the effects of loss of Erg29 on sterol synthesis. Δ*erg29pGAL1ERG29* cells grown in galactose had some increase in the levels of 4,4-DMZ and 4-methyl fecosterol and decreased levels of ergosterol compared with WT cells; however, in glucose-containing medium, Δ*erg29pGAL1ERG29* cells showed an increase in intermediate sterols and a corresponding decrease in zymosterol and ergosterol (Fig. 1*B*). We confirmed that growth in glucose resulted in the loss of Erg29-His protein (Fig. 1*C*). We note that WT cells grown in glucose accumulated more zymosterol than when grown in galactose. We do not know the reason for this observation. We hypothesize that the altered sterols seen in galactose-grown Δ*erg29pGAL1ERG29* cells reflect decreased function of the epitope-tagged Erg29. We confirmed this hypothesis by transforming the Δ*erg29p*β-*estradiolGAL1ERG29* strain with a plasmid containing non-tagged *ERG29* under its endogenous promoter. Sterol analysis revealed lower levels of methyl sterol intermediates and increased zymosterol and ergosterol in cells expressing nontagged Erg29 (Fig. 1*D*). This supports the hypothesis that the epitope tag reduced the function of Erg29. We also determined that the untagged Erg29 functioned better in complementing the loss of Erg29 (Fig. 1*D*, + *pYcp ERG29* + β-estradiol (*hatched gray bar*) compared with +β-estradiol alone (*gray bar*)).

The sterol pattern observed in *ERG29* "shut-off" cells was similar to that seen in cells with mutations in *ERG25* (18). To more closely examine the similarities in sterol profiles, we generated a *ERG25* deletion strain expressing a β-estradiol *pGAL1ERG25* similar to the "*ERG29* shut-off" system. Δ*erg25pGAL1ERG25* cells grown in galactose had some increase in the levels of 4,4-DMZ and 4-methyl fecosterol and decreased levels of ergosterol compared with WT cells; however, in glucose-containing medium Δ*erg25pGAL1ERG25* cells showed a dramatic increase in 4,4-DMZ and a corresponding decrease in zymosterol and ergosterol (Fig. 1*E*). We confirmed that growth in glucose resulted in the loss of Erg25 protein (Fig. 1*C*). The sterol pattern seen in glucose-grown Δ*erg25pGAL1ERG25* cells appears similar to that in Δ*erg29pGAL1ERG29* cells, although we consistently observed higher levels of the methyl sterol intermediates, such as 4-methyl fecosterol (see Fig. 1*B*) and 4-carboxyzymosterol in Δ*erg29pGAL1ERG29* cells (data not shown). That the loss of *ERG29* affects the methyl sterol oxidase reaction is supported by the observation that overexpression of *ERG25*, through transformation with a high-copy plasmid permitted Δ*erg29* cells to survive (Fig. 2*A*). In contrast, transformation with a high-copy *ERG26* plasmid, which encodes the subsequent enzyme in the methyl sterol oxidase reaction (21), did not. Together, the results support the hypothesis that the loss of *ERG29* affects the methyl sterol oxidase reaction in which Erg25 is the first enzyme in the reaction. These results suggest that the "shut-off" of *ERG29* specifically affects the Erg25 reaction and not another enzyme in the methyl sterol oxidase reaction. Erg25 is localized to the endoplasmic reticulum (18). We generated a MET3-regulated ERG29-GFP plasmid and transformed it into WT or Δ*erg29pGAL1ERG29* cells. We confirmed that the carboxyl-tagged Erg29-GFP complemented the loss of *ERG29* (Fig. 2*B*) and confirmed that Erg29-GFP is localized to
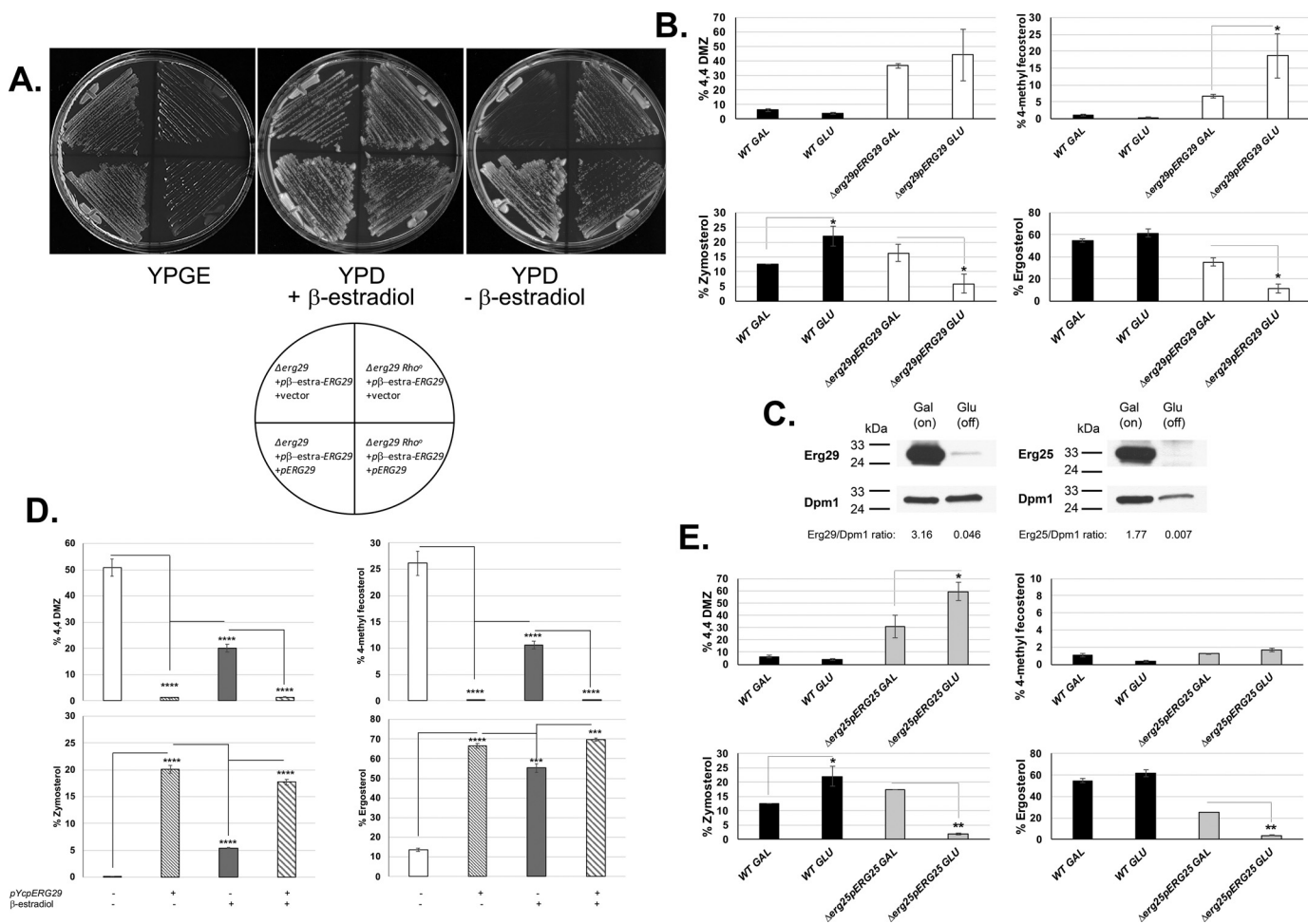
ASBMB

J. Biol. Chem. (2018) 293(27) 10782–10795 **10783**

Figure 1. Loss of *ERG29* results in loss of the mitochondrial genome and increased levels of 4,4-DMZ and 4-methyl fecosterol. *A*, Δ*erg29pβ-estradiolGAL1ERG29* (Rho⁺ or Rho⁰ (spontaneous Rho⁰)) containing empty vector pYCp or pYCp*ERG29* cells were grown on YPGE or YPD plates in the presence or absence of β-estradiol for 4 days. *B*, WT (DY1457*pβ-estradiolGAL1* vector) and Δ*erg29pβ-estradiolGAL1ERG29* were grown in galactose or glucose for 16 h, sterols were extracted, and sterol analysis was performed using GC/MS as described under "Materials and methods." The data are expressed as the percentage of total sterols. *Error bars*, S.D. $n = 3$. *C*, Western blot analysis of Erg29-HIS or Erg25 protein levels in galactose and glucose was performed using His$_6$ antibody or Erg25 antibody as described under "Materials and methods". Dpm1, an ER protein, was used as a load control. $n = 3$. A representative blot is shown. The ratio of Erg29 or Erg25 to Dpm1 was determined using Bio-Rad ImageLab™ software. *D*, Δ*erg29pβ-estradiolGAL1ERG29* containing either empty vector or pYCp*ERG29* cells was grown in glucose in the absence or presence of β-estradiol for 16 h, and sterol analysis was performed as described in *B*. The data are expressed as the percentage of total sterols. *Error bars*, S.D. of four replicates. *White bars*, no Erg29; *white hatched bars*, *ERG29* expressed under its endogenous promoter; *gray bars*, +β-estradiol ERG29 expression; *gray larger hatched bars*, +β-estradiol ERG29 expression and *ERG29* expressed under its endogenous promoter. *E*, WT (DY1457*pβ-estradiolGAL1* empty vector) and Δ*erg25 pGALERG25* cells were grown in galactose- or glucose-containing medium for 16 h as in *B*, and sterol analysis was performed as described. The Δ*erg25* samples were prepared, and sterol analysis was done in the same experiment as *B* to contrast Δ*erg29* and Δ*erg25*; therefore, the WT data shown is the same in *B* and *E*. The data are expressed as the percentage of total sterols. *Error bars*, S.D. $n = 3$.

the endoplasmic reticulum (Fig. 2C) similar to that reported in a previous genomic epitope tag study (22).

Loss of respiration affects the sterol pattern in Δerg29 cells

As described in Fig. 1, loss of respiration can permit Δ*erg29* cells to survive as Rho⁰ cells. Based on this result, we examined whether there were changes in the sterol pattern in Rho⁰ cells. We used ethidium bromide to generate Rho⁰ WT cells and then deleted *ERG29* to generate Δ*erg29* Rho⁰ cells. Making cells Rho⁰ alone did not affect ergosterol synthesis, whereas the loss of *ERG29* in Rho⁰ cells showed diminished ergosterol synthesis and increased intermediate sterols compared with WT Rho⁰ cells (Fig. 3A); however, the levels of accumulated intermediates were reduced in Δ*erg29* Rho⁰ cells compared with Δ*erg29pGAL1ERG29* grown in glucose (Fig. 1B) or in the absence of β-estradiol (Fig. 1C). Further, the amount of ergos-

terol synthesized in Δ*erg29* Rho⁰ cells was increased compared with Δ*erg29pGAL1ERG29* grown in glucose or in the absence of β-*estradiol*. These results suggest that mitochondrial respiration or mitochondrial oxidants affect ergosterol synthesis in the absence of *ERG29*.

To determine whether iron limitation affected sterol synthesis, WT Rho⁰ and Δ*erg29* Rho⁰ cells were grown in medium made iron-limited by the iron chelator bathophenanthroline sulfonate (BPS). Δ*erg29* Rho⁰ cells grew poorly (BPS with 0–4 μM iron (*BPS(0)* to *BPS(4)*) but equal to WT Rho⁰ cells with increased iron (*BPS(100)*)) (Fig. 3B). As Δ*erg29* Rho⁰ cells grew poorly if grown on iron-limited medium for extended times, we grew WT Rho⁰ and Δ*erg29* Rho⁰ cells in iron-limited medium for 4 h to examine whether limiting iron affected sterol synthesis. Δ*erg29* Rho⁰ cells still showed increased intermediate sterols (4,4-DMZ and 4-methyl fecosterol) and reduced zymos-

A.

$\Delta erg29pGAL1ERG29$

Galactose   Glucose

empty vector

pYEpERG25

pYEpERG26

B.

Galactose (on)   Glucose -M (off)

empty vector

ERG29-GFP
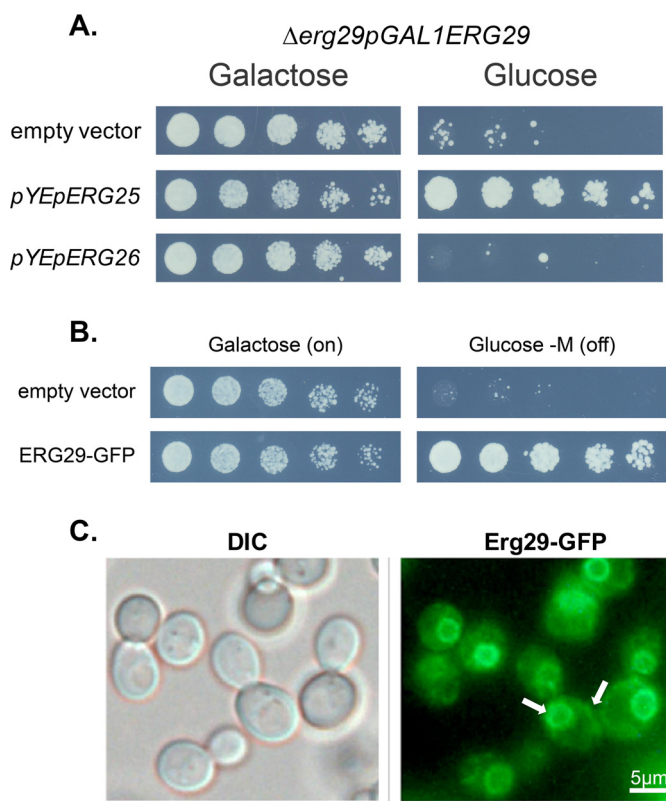
C.

DIC   Erg29-GFP

5μm

Figure 2. Erg25 partially suppresses the loss of ER-localized Erg29. *A*, $\Delta erg29p\beta$-*estradiolGAL1ERG29* transformed with pYEp, pYEp*ERG25*, or pYEp*ERG26* was grown in galactose or glucose for 3 days. *B*, $\Delta erg29p\beta$-*estradiolGAL1ERG29* transformed with *pMET3YEp* or *pMET3ERG29-GFP* was grown in galactose or glucose minus methionine for 2 days. *C*, WT cells were transformed with a complementing plasmid containing MET3*ERG29*-GFP. The cells were grown to mid-log phase in the absence of methionine and examined by epifluorescence microscopy as described under "Materials and methods." *Arrows*, typical ER localization surrounding the nucleus and near the plasma membrane similar to Erg25 localization (18). *DIC*, differential interference contrast.

terol and ergosterol synthesis compared with WT Rho^0 cells (Fig. 3*C*). These results demonstrate that short-term growth in iron-limited medium did not affect the altered sterols seen in $\Delta erg29$ cells.

Loss of Erg29 affects the methyl sterol oxidase reaction

$\Delta erg29$ Rho^0 cells were much more sensitive to conditions that affected the methyl sterol oxidase reaction than WT Rho^0 cells. Incubation of cells with cobalt has been shown to inhibit the enzyme activity of oxo-diiron–containing Erg25 in both *Saccharomyces cerevisiae* and *Cryptococcus neoformans*, leading to a hyperaccumulation of 4,4-DMZ and decreased levels of zymosterol (23). The addition of 1.0 mm cobalt to WT Rho^0 cells had little effect on viability, whereas $\Delta erg29$ Rho^0 cells showed a loss of viability (Fig. 3*D*). Further, we utilized the Erg25 inhibitor 6-amino-2-*n*-pentylthiobenzothiazole (APB) to assess growth of $\Delta erg29$ Rho^0 cells. WT Rho^0 cells showed some toxicity at 60 μM APB, whereas $\Delta erg29$ Rho^0 cells showed toxic effects at 20 μM (Fig. 3*E*). These results support the view that loss of *ERG29* increases the sensitivity of Erg25 to agents known to affect the Erg25 reaction. Together, these results strongly support the hypothesis that Erg29 functions in the Erg25 methyl sterol

oxidase reaction and that mitochondrial respiration affects ergosterol synthesis.

Identification of genetic suppressors of ERG29

We took a genetic approach to examine the mechanism of toxicity due to loss of *ERG29*. As loss of *ERG29* results in death when cells are grown in respiratory medium, we used a high-copy genomic library (*LEU2*) to identify suppressors that would permit growth of $\Delta erg29$ cells on glycerol-ethanol (GE). We transformed our $\Delta erg29YCpERG29(URA3)$ strain with a genomic library. We then selected for loss of YC*pERG29* on 5-fluoroorotic acid and identified surviving colonies that could grow on GE. As expected, several recovered plasmids that allowed $\Delta erg29$ Rho$^+$ cells to grow on GE contained the *ERG29* gene (data not shown). In addition, we found *MMT2*, *YFH1*, and *PET20* as high-copy suppressors. That we did not recover ERG25 as a high-copy suppressor suggests that our screen was not saturated. We confirmed that overexpression of *MMT2*, *YFH1*, and *PET20* permitted *ERG29* shut-off ($\Delta erg29pGAL1ERG29$) cells to grow on glucose (Fig. 4*A*). Babcock *et al.* (4) initially identified *YFH1* as a high-copy suppressor of the missense mutant Erg29 (*bm-8*) (4). Our results show that *YFH1* can also partially suppress the growth defect of $\Delta erg29$ cells. *MMT2* encodes a mitochondrial iron exporter, which is a member of the family of cation diffusion facilitators (24, 25). *MMT2* has a paralogue, *MMT1*. We did not find *MMT1* in our screen, but we confirmed that overexpression of *MMT1* would permit $\Delta erg29$ cells to grow as Rho$^+$ (Fig. 4*A*). *PET20* is a nuclear gene that encodes a mitochondrial protein, which when deleted leads to increased sensitivity to oxidant stress (15). All of the plasmids that permitted growth of $\Delta erg29$ cells also affected the $\Delta erg29$ sterol pattern (Fig. 4*B*). Overexpression of these genes did not normalize the sterol pattern of *ERG29* shut-off cells but did reduce the levels of 4,4-DMZ and 4-methyl fecosterol and concomitantly increased the levels of zymosterol and ergosterol.

The finding that the overexpression of mitochondrial iron exporter genes *MMT1* and *MMT2* preserved the respiratory activity of a $\Delta erg29$ led us to examine the effect of either deletion or overexpression of the mitochondrial iron importer genes *MRS3* and *MRS4*. Deletion of *MRS3* and *MRS4* together but not singly permitted $\Delta erg29$ cells to grow on GE medium (Fig. 5*A*, *right plate*, *bottom panels*). We observed that overexpression of *MRS3* in $\Delta mrs3\Delta mrs4$ cells did not affect viability (Fig. 5*A*, *left plate*, *top panels*), whereas overexpression of *MRS3* in $\Delta mrs3\Delta mrs4\Delta erg29$ cells resulted in a loss of viability on GE medium (Fig. 5*A*, *left plate*, *bottom panels*). Indeed, overexpression of *MRS3* in $\Delta erg29$ Rho^0 cells led to increased levels of 4,4-DMZ and 4-methyl fecosterol and decreased zymosterol and ergosterol (Fig. 5*B*). The effects of *MRS3* were suppressed if the mitochondrial iron exporter *MMT1* was overexpressed at the same time. These results suggest a connection between mitochondrial iron levels, loss of viability, and high levels of methyl sterol intermediates.

Loss of ERG29 affects Fe-S cluster synthesis

Increased *MRS3* expression affects cell growth of $\Delta erg29$ cells, whereas overexpression of *MMT1* or deletion of *MRS3*/
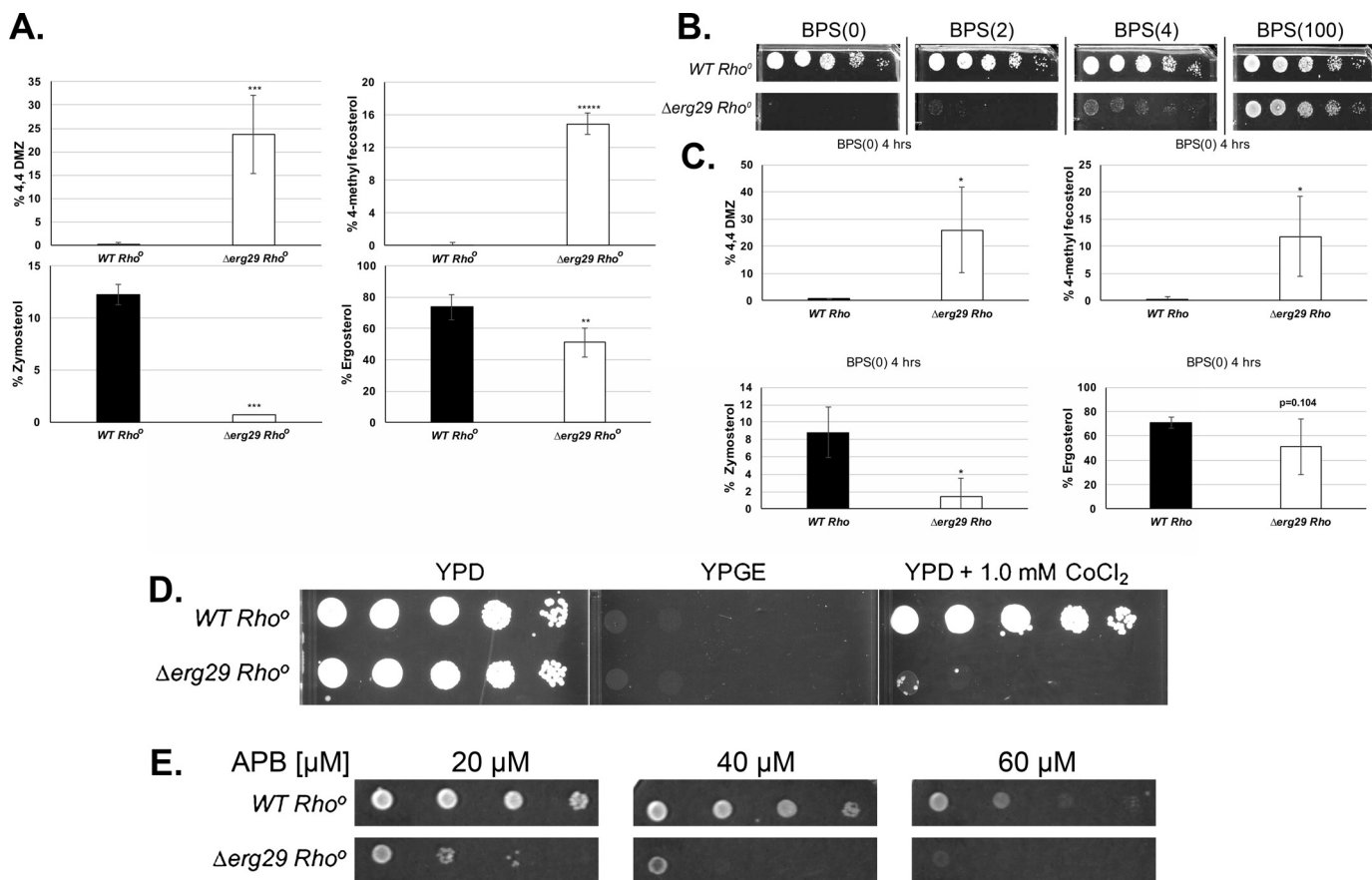
Figure 3. Loss of respiration affects the sterol pattern of Δerg29 cells. *A*, WT Rho^0 and Δ*erg29* Rho^0 cells were grown in CM glucose medium for 18 h, and sterol analysis was performed as described. The data are expressed as the percentage of total sterols. *Error bars*, S.D. of four separate experiments. *B*, cells as in *A* were plated onto iron-limited medium (BPS (0–100 μM iron)) and grown at 30 °C for 2 days. *C*, sterol analysis was performed on cells grown in iron-limited medium (BPS(0)) for 4 h. The data are expressed as the percentage of total sterols. *Error bars*, S.D. of two separate experiments. *D*, cells as in *A* were plated onto YPD with or without 1 mM CoCl$_2$ or YPGE and grown at 30 °C for 3 days. *E*, cells as in *A* were plated onto CM medium containing varying concentrations (μM) of ABP and grown at 30 °C for 2 days.

MRS4 protects these cells. Similar findings have been reported in cells with a deletion in *YFH1*. Most notably, the growth of Δ*yfh1* cells was reduced by overexpression of *MRS3* or *MRS4* but protected by deletion of these genes (26–29). We confirmed that overexpression of *MMT1* permitted Δ*yfh1* cells to grow in medium supplemented with iron or H$_2$O$_2$ (Fig. 6*A*). Loss of Yfh1 is known to decrease Fe-S cluster synthesis, which leads to the accumulation of iron in mitochondria as ferric iron deposits (5, 29–31). Together, these findings suggest that the accumulation of methyl sterol intermediates may also lead to loss of mitochondrial Fe-S cluster synthesis. We tested this hypothesis by measuring the activity of the Fe-S–containing mitochondrial aconitase in Δ*erg29pGAL1ERG29* cells. In the presence of glucose, *ERG29* shut-off, there was a dramatic decrease in aconitase activity in Δ*erg29pGAL1ERG29* cells compared with WT cells (Fig. 6*B*). Overexpression of the high-copy suppressor *YFH1*, *MMT1*, *MMT2*, or *PET20* in Δ*erg29*pGAL1*ERG29* cells grown in glucose resulted in improved aconitase activity.

Lipoate synthase is an Fe-S cluster–containing protein, which is rapidly degraded in the absence of Fe-S clusters, resulting in decreased lipoic acid modifications to mitochondrial proteins (32–34). Measuring lipoic acid modification on proteins by Western blotting provides a measure of Fe-S synthesis.

ERG29 shut-off resulted in decreased lipoic acid modifications on pyruvate dehydrogenase (*PDH*) and oxoketoglutarate dehydrogenase (*KDH*) (35, 36), whereas overexpression of *YFH1*, *MMT1*, *MMT2*, or *PET20* in Δ*erg29pGAL1ERG29* cells resulted in a partial recovery of lipoic acid modifications (Fig. 6*C*). Together, these results confirm that loss of *ERG29* affects mitochondrial Fe-S cluster synthesis.

Loss of ERG29 in respiratory cells affects Yfh1 levels

Yfh1 affects an early step in the synthesis of Fe-S clusters within mitochondria. The observation that loss of *ERG29* can be suppressed by overexpressed *YFH1* led us to examine the levels of Yfh1 in respiring cells when *ERG29* was "shut off." Isolation of mitochondria from Δ*erg29pGAL1ERG29* cells grown in glucose showed a decrease in the level of Yfh1 (Fig. 7*A*, *lane 6*), which was not due to a reduction in *YFH1* mRNA levels (Fig. 7*B*). In fact, *YFH1* transcripts were up-regulated slightly in response to loss of Erg29, whereas *ISU1* transcripts were unaltered. The decrease in Yfh1 protein was specific to Yfh1, as little or no decrease was observed in other Fe-S cluster synthesis proteins, including Nfs1, the cysteine desulfurase involved in generating sulfide (37, 38); Isu1, a Fe-S scaffold protein (39); and Ssq1, a chaperone involved in the assembly of mitochondrial Fe-S clusters (40, 41). Overexpression of *MMT1* or *PET20*
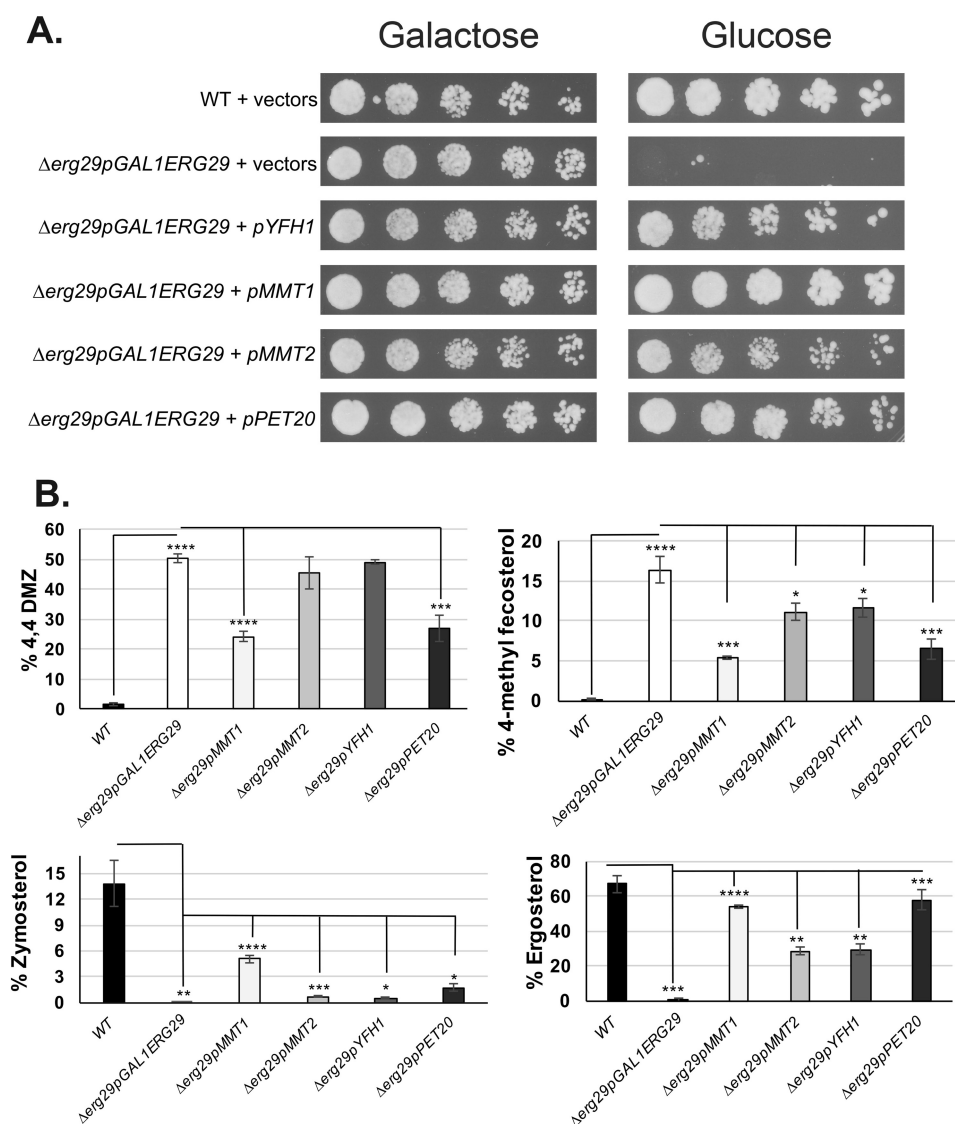
A.

B.

Figure 4. Library screen identifies *YFH1*, *MMT1*, *MMT2*, and *PET20* as high-copy suppressors of the loss of *ERG29*. *A*, WT cells containing pYEp or Δ*erg29pGAL1ERG29* cells transformed with pYEp or identified library candidates (*YFH1*, *MMT1*, *MMT2*, or *PET20*) were plated onto galactose- or glucose-containing medium and grown for 3 days. $n = 4$. *B*, sterol analysis was performed on cells as in *A*, grown in glucose-containing medium for 18 h. The data are expressed as the percentage of total sterols. *Error bars*, S.D. $n = 3$.

in Δ*erg29pGAL1ERG29* cells permitted partial rescue of Yfh1 levels. We note that overexpression of *PET20* affected the levels of Isu1 in both galactose- and glucose-grown cells. We do not know the reason for this reduction but note that the reduction in Isu1 did not affect aconitase activity.

Loss of ERG29 leads to increased mitochondrial oxidants

Under normal conditions, increased pools of free mitochondrial iron do not impose a growth deficit in cells (42). Under conditions of stress or specific gene deletions, however, pools of free mitochondrial iron exacerbate the generation of oxidant radicals (43, 44). Based on those findings, we examined whether loss of *ERG29* led to increased mitochondrial oxidants using the reagent MitoSOX Red, which localizes to mitochondria and upon oxidation becomes fluorescent. WT cells showed a low level of mitochondrial oxidants, whereas Δ*erg29pGAL1ERG29* cells grown in glucose medium showed a dramatic increase in mitochondrial oxidants (Fig. 7*C*). This increase was signifi-

cantly reduced by overexpression of *YFH1*, *MMT1*, *MMT2*, or *PET20*. These results confirm that loss of *ERG29* increases mitochondrial oxidants and that altering mitochondrial iron either through increased iron export or by increasing Fe-S cluster synthesis reduces mitochondrial oxidants.

Loss of ERG25 affects mitochondrial activities

The finding that loss of *ERG29* affects mitochondrial activities prompted us to test the effects of loss of *ERG25* on mitochondrial activity, because both genes affect the methyl sterol oxidase reaction. Δ*erg25pGAL1ERG25* cells grown in glucose showed decreased aconitase activity compared with WT cells (Fig. 8*A*), decreased Yfh1 levels (Fig. 8*B*), and increased mitochondrial oxidants (Fig. 8*C*). Neither the growth phenotype (data not shown) nor changes in mitochondrial activity due to "shut-off" of *ERG25* could be suppressed by overexpression of *MMT1*, *MMT2*, or *YFH1*. As Erg25 is an essential enzyme, these results suggest that the effects of complete Erg25 loss

A.

GE

-Met (ON)

Δmrs3Δmrs4
pMET3MRS3

Δmrs3Δmrs4Δerg29
pMET3MRS3

+Met (OFF)

Δmrs3Δmrs4
pMET3MRS3
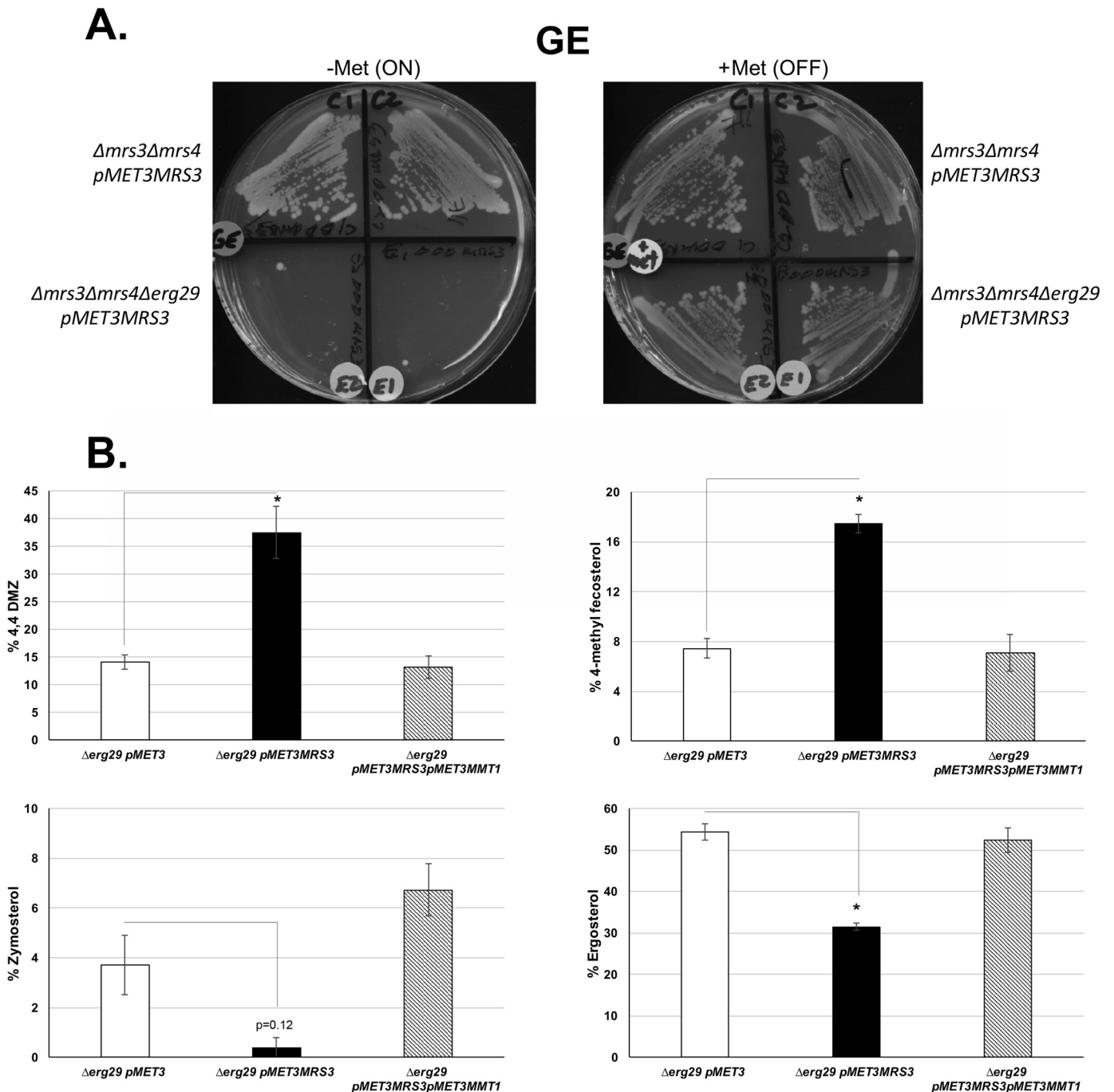
Δmrs3Δmrs4Δerg29
pMET3MRS3

B.

Figure 5. Changes in mitochondrial iron levels affect Δ*erg29* growth on respiratory substrates. *A*, two separate clones of either Δ*mrs3*Δ*mrs4* (C1/C2) or Δ*erg29*Δ*mrs3*Δ*mrs4* (E1/E2) containing a p*MET3MRS3* plasmid were grown on GE-containing medium + 10× Met (*OFF*) or −Met (*ON*) for 5 days. *n* = 2. *B*, Δ*erg29* Rho⁰ cells containing p*MET3*, p*MET3MRS3*, or p*METMRS3* and p*MET3MMT1* were grown in the absence of methionine for 8 h, and sterol analysis was performed. The data are expressed as the percentage of total sterols. *Error bars*, S.D. of two separate experiments.

cannot be overcome by simply altering mitochondrial iron levels or Fe-S cluster synthesis.

Discussion

The results reported here suggest that Erg29 is involved in sterol metabolism and that loss of Erg29 results in the generation of 4-methyl sterol metabolites. Data suggesting that Erg29 is involved in sterol metabolism include the following: 1) Erg29 is localized to the ER, where methyl sterol synthesis occurs; 2) loss of *ERG29* affects the methyl sterol oxidase reaction, result-

ing in increased levels of 4,4-DMZ and 4-methyl sterol intermediates and correspondingly decreased levels of zymosterol and ergosterol; and 3) Δ*erg29* Rho⁰ cells are more sensitive than WT cells to agents that affect the methyl sterol oxidase reaction. These data, most notably the accumulation of 4,4-DMZ, the loss of zymosterol and ergosterol, and suppression by overexpression of *ERG25* point to the methyl sterol oxidase reaction being affected in Δ*erg29* cells, although the exact role of Erg29 is unclear. The finding that Erg29 affects the sterol pathway is supported by data presented in large chemogenomic studies
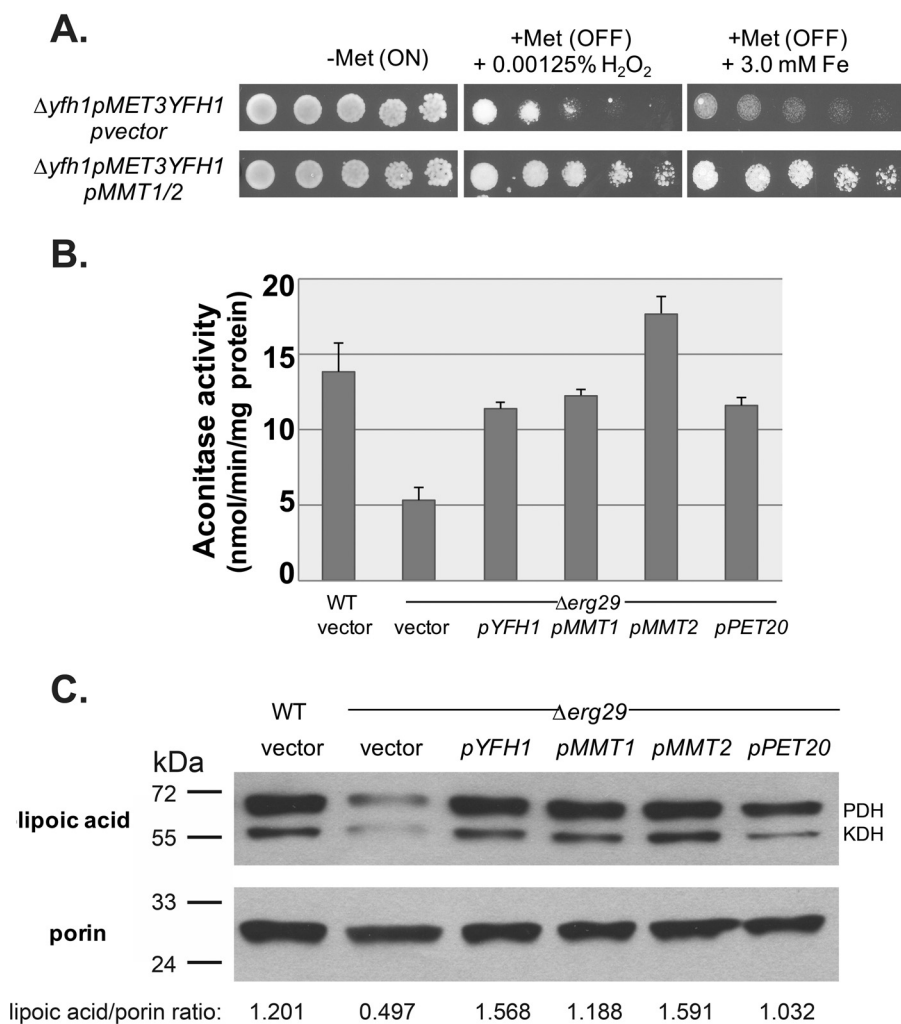
ASBMB

Figure 6. Loss of *YFH1* or *ERG29* affects Fe-S cluster synthesis. *A*, Δ*yfh1pMET3YFH1* cells containing empty vector or p*MMT1/2* were grown on CM plus (*OFF*) or minus 10× methionine (*ON*) with or without 0.00125% H$_2$O$_2$ or 3.0 mM iron (*Fe*) for 3 days. *B*, WT 1457 and Δ*erg29* p*GAL1ERG29* cells with empty vector, p*YFH1*, p*MMT1*, p*MMT2*, or p*PET20* were grown in glucose for 18 h, and aconitase activity was measured as described under "Materials and methods." *n* = 3. *C*, lysates from *B* were analyzed for lipoic acid protein modification by Western blotting as described previously (35). *n* = 3. *PDH*, pyruvate dehydrogenase; *KDH*, α-ketogluterate dehydrogenase. The ratio of lipoic acid modification/porin was determined using Bio-Rad ImageLab™ software. *Error bars*, S.D.

(45, 46). We were unable to suppress the loss of *ERG29* through the addition of ergosterol even in cells overexpressing the Sut1 transcription factor that up-regulates sterol uptake genes (47, 48) (data not shown). Similarly, Lee *et al.* (46) reported that the addition of ergosterol did not rescue the growth defect associated with Erg29-specific inhibitors. These results suggest that it is not the loss of ergosterol that results in toxicity but rather the accumulation of intermediate sterols. A similar finding was reported for loss of *ERG26* or a temperature-sensitive allele of *erg26-1* in which ergosterol supplementation could not overcome toxicity (21, 49). The exact role of Erg29 in the methyl sterol oxidase reaction remains to be identified. We hypothesized that Erg29 may be acting to deliver iron to Erg25 or that it may be a chaperone for Erg25, although extensive experimentation has not shown iron bound to Erg29, and we have been unsuccessful in co-immunoprecipitating Erg29 and Erg25 (data not shown).

We have not identified the specific toxic sterol intermediates generated when *ERG29* is lost, but our data suggest that their levels are affected by oxidants. Reductions in mitochondrial

respiration (Rho[0]), or reduction of mitochondrial iron-based oxidants led to suppression of toxicity and at least a partial restoration of sterol metabolism. The genetic suppressors did not return the sterol profile to normal but did decrease the accumulation of 4,4-DMZ and 4-methyl fecosterol. Loss of *ERG25* led to a similar constellation of phenotypes (decreased Fe-S synthesis, increased mitochondrial oxidants, and loss of Yfh1). These phenotypes, however, could not be suppressed by overexpression of those genes that suppressed the Δ*erg29* phenotype. These results suggest that loss of Erg29 makes the methyl sterol oxidase reaction sensitive to oxidized sterol intermediates. Most of the oxidation of the sterols is due to reactive oxygen present in the mitochondria either as a result of respiration or the interaction of reactive sterol metabolites with iron, leading to a further increase in reactive oxygen. In the absence of mitochondrial respiration (Rho[0]), however, other conditions that lead to increased oxidants, such as decreased mitochondrial iron transport (43) or increased cobalt (23), may result in more oxidized sterols and an attack on Fe-S clusters. Many of the enzymes involved in Fe-S cluster synthesis are themselves
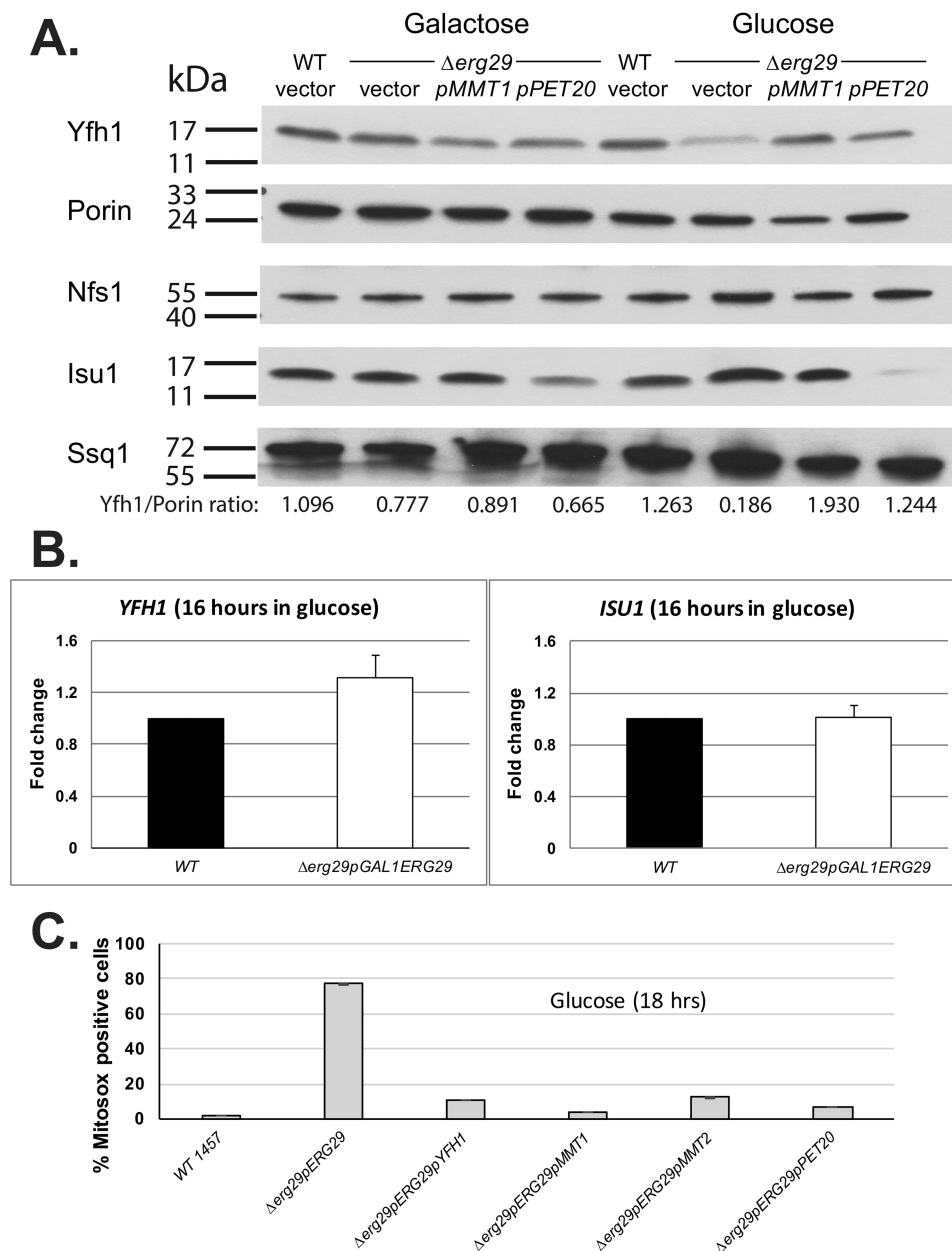
Figure 7. Loss of *ERG29* results in decreased levels of Yfh1 protein and increased mitochondrial oxidants. *A*, mitochondrial preparations from WT*pYEp*, Δ*erg29pGAL1ERG29pYEp*, p*MMT1*, or p*PET20* grown in galactose or glucose were analyzed for Yfh1, porin, Nfs1, Isu1, and Ssq1 by Western blotting. *n* = 2. Gels were quantified using Bio-Rad ImageLab™ software with Yfh1 levels normalized to porin in each sample. *B*, mRNA was isolated from WT*pYEp* or Δ*erg29* p*GAL1ERG29* cells grown in glucose for 16 h, and quantitative PCR was performed for *YFH1* or *ISU1* and *ACT1* for normalization. *C*, cells as in *B* were incubated with 20 nM Mitosox dye and washed, and Mitosox fluorescence was determined by flow cytometry in duplicate as described under "Materials and methods." *n* = 2 separate experiments. *Error bars*, S.D.

Fe-S cluster–containing enzymes. The nature of the genetic suppressors identified in this study supports the model that exporting iron through Mmt1 and Mmt2 will reduce oxidant generation. Yfh1 may be the target for reactive oxidants, which results in its degradation. It is also possible that *YFH1* translation may be decreased, resulting in decreased levels of Yfh1 protein. We have not formally addressed this possibility in the current studies. We found that overexpression of *YFH1* results in increased Yfh1 in mitochondria, yet it only showed mild suppression of the sterol intermediate accumulation seen in Δ*erg29* cells. It may be that oxidized Yfh1 is functionally inactive or that Yfh1 suppresses the Δ*erg29* phenotype by chelating iron, as

Yfh1 has been suggested to be an iron-binding protein (8, 11, 50). The function of Pet20 is unclear except that its loss renders respiratory active yeast susceptible to a wide variety of conditions, including H_2O_2 and the antifungal drug fluconazole (15).

In otherwise normal cells, increases in the mitochondrial free iron pool do not affect cell growth. Indeed, overexpression of *MRS3* or *MRS4* can rescue the cytosolic iron lethality due to loss of the vacuolar iron importer Ccc1 (43). To our knowledge, it is only under conditions in which mitochondrial Fe-S cluster synthesis is diminished that increased mitochondrial iron is toxic. Loss of Fe-S synthesis results in the formation of iron
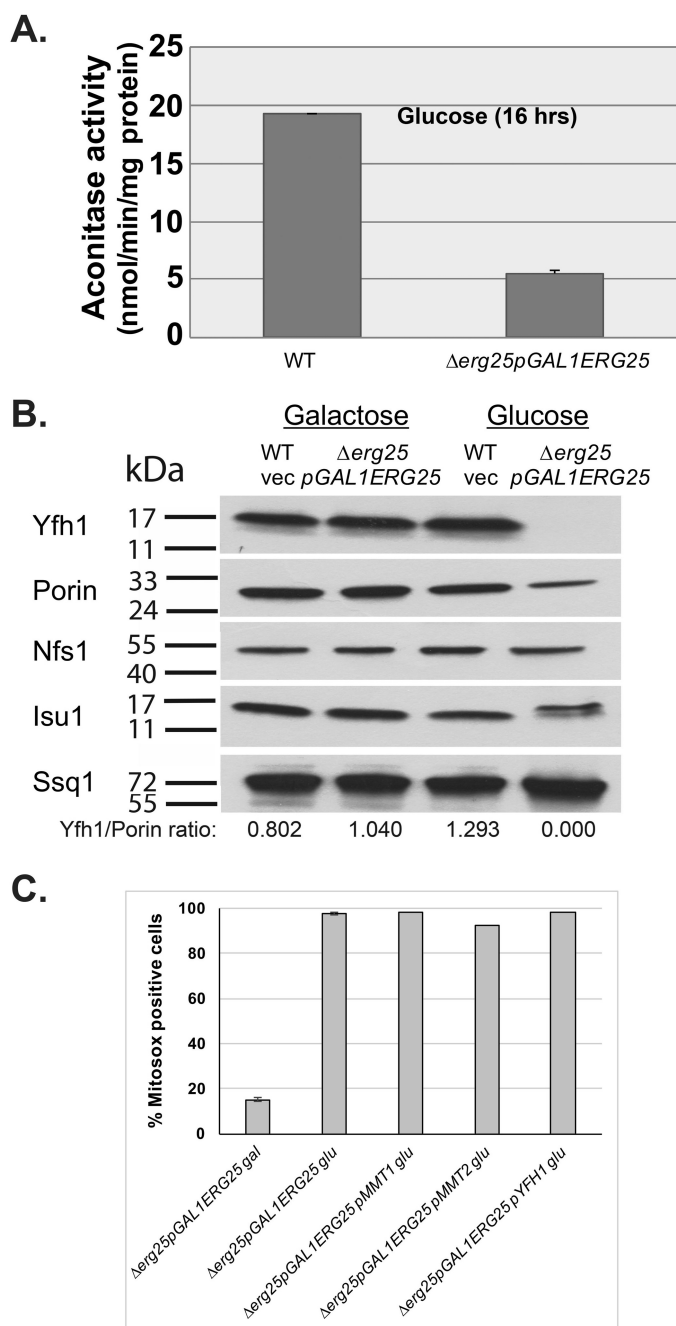
A.

B.

C.

Figure 8. Loss of *ERG25* results in decreased Fe-S synthesis and decreased Yfh1. *A*, WT and Δ*erg25pGAL1ERG25* cells were grown in glucose-containing medium for 16 h, and aconitase activity was measured. *n* = 2 with two separate clones per experiment. *B*, mitochondrial lysates from cells as in *A* grown in galactose or glucose were analyzed for Yfh1, porin, Nfs1, Isu1, and Ssq1by Western blotting. Gels were quantified using Bio-Rad ImageLab™ software with Yfh1 levels normalized to porin in each sample. *C*, Δ*erg25pGAL1ERG25* containing pYEp, p*MMT1*, p*MMT2*, or p*YFH1* grown in galactose or glucose for 16 h was incubated with 20 nM Mitosox dye and washed, and Mitosox fluorescence was determined by flow cytometry in duplicate as described under "Materials and methods." *n* = 2.

nanoparticles, presumably by an oxidation step. Reducing the generation of iron nanoparticles by restricting the free iron pool reduces oxidant generation and the deleterious effects of those oxidants (11). The findings reported here all support the idea that generation of methyl sterol metabolites results in mitochondrial oxidation linked to iron, which then affects the essen-

tial Fe-S cluster biosynthetic process. The generation of sterol metabolites precedes the loss of Fe-S cluster activity, as decreasing Fe-S cluster activity by reducing the levels of Yfh1 or Nfs1 does not result in altered sterols (51).

Other reports show a relationship between altered sterol biosynthesis and mitochondrial Fe-S cluster synthesis. Fluconazole is an azole derivative that affects the reaction catalyzed by Erg11 (52), an ER-localized sterol synthesis enzyme. The toxicity of fluconazole is due to the generation of sterol intermediates, which can be affected by mitochondrial respiration, resulting in the generation of toxic 4-methyl sterol intermediates. Most recently, Demuyser *et al.* (53) identified the mitochondrial chaperone protein Mge1 as a high-copy suppressor of fluconazole toxicity. Mge1 is a chaperone involved in Fe-S cluster metabolism and protein import into the mitochondria. The authors showed that Mge1 acted as a suppressor by increasing ergosterol upon fluconazole treatment and that the suppressive effect of Mge1 overexpression was lost in cells that had a deletion in the Fe-S chaperone encoded by *SSQ1*, pointing again to involvement of Fe-S synthesis in the toxicity of fluconazole.

The finding that Yfh1 and Fe-S cluster synthesis may be a target for mitochondrial oxidants may extend to agents other than sterol metabolites and to species other than yeast. It is well established that doxorubicin-induced cardiac toxicity is due to the generation of iron-related oxidants (54, 55). Expression of mitochondrial ferritin can protect HeLa cells from doxorubicin toxicity (56), and mice with a targeted gene deletion in mitochondrial ferritin are much more sensitive to doxorubicin-mediated cardiac toxicity than normal mice (57). Ardehali and colleagues (58) reported that overexpression of Abcb8, a mitochondrial ATP transporter, reduced doxorubicin-mediated toxicity. The substrate transported out of the mitochondria by Abcb8 was a Fe-GSH conjugate, although the exact compound was unclear. Recently, Mouli *et al.* (59) reported that doxorubicin induced the loss of Fe-S cluster synthesis by reducing the levels of frataxin in cultured cardiac myocytes due to increased degradation. They also showed that overexpression of frataxin prevents doxorubicin toxicity. Overexpression of frataxin in transgenic flies suppressed the effects of iron, H_2O_2, and paraquat on lifespan (60). Further studies demonstrated that a purified recombinant cell-permeable frataxin (PEP1-frataxin) protected neuronal cells from oxidant-mediated cell death (61). The effects of the Parkinson's disease-inducing neurotoxin 1-methyl-4-phenyl-1,2,3,6-tetrahydropyridine, which targets complex I in the electron transport chain, can be suppressed by overexpression of ferritin or through increased levels of frataxin due to administration of Tat-frataxin (62). These results underscore that mitochondria are highly susceptible to iron-mediated toxicity and suggest that this toxicity may target Fe-S cluster formation. The data also suggest that frataxin may be a central target for oxidants either due to its specific role in Fe-S cluster synthesis or as an iron-binding molecule. Based on these findings, we speculate that other compounds that result in mitochondrial toxicity, through generation of reactive oxygen radicals, might also attack Fe-S cluster synthesis and be suppressed by either removal of mitochondrial iron or increased levels of frataxin.

ASBMB

J. Biol. Chem. (2018) 293(27) 10782–10795 **10791**

Table 2
Yeast strains used in this study

Strain	Genotype	Source/Reference
DY1457	*ura3-52, leu2-3,112, trp1-1, his3-11, 15, ade6, can1-100(oc)*	Ref. 42
DY150	*ura3-52, leu2-3, 112, trp1-1, ade2-1, can1-100(oc)*	Ref. 42
Δ*erg29pβ-estradiol (pGEV)pGAL1ERG29*	*ura3-52, leu2-3,112, trp1-1, his3-11, 15, ade6, can1-100(oc)*	This study
	Δ*erg29::KanMX4 pβ-estradiol-pGAL1ERG29–6XHIS*	
Δ*erg25pβ-estradiol (pGEV)pGAL1ERG25*	*ura3-52, leu2-3,112, trp1-1, his3-11, 15, ade6, can1–100(oc)*	This study
	Δ*erg25::KanMX4 pβ-estradiol-pGAL1-ERG25–6XHIS*	
DY1457 Rho⁰	*ura3-52, leu2-3,112, trp1-1, his3-11, 15, ade6, can1-100(oc)*	This study
Δ*erg29* Rho⁰	*ura3-52, leu2-3,112, trp1-1, his3-11, 15, ade6, can1-100(oc) Δerg29::KanMX4*	This study
Δ*yfh1MET3YFH1*	*ura3-52, leu2-3, 112, trp1-1, ade2-1, can1-100(oc), Δyfh1::HIS3*	Refs. 5 and 51
Δ*mrs3Δmrs4*	*ura3-52, leu2-3, 112, trp1-1, ade2-1, can1-100(oc), Δmrs3Δmrs4::KAN*	Refs. 42, 67, and 68
Δ*mrs3Δmrs4Δerg29*	*ura3-52, leu2-3, 112, trp1-1, ade2-1, can1-100(oc), Δerg29::HIS3, Δmrs3Δmrs4::KAN*	This study

Materials and methods

Yeast, plasmids, and growth medium

Genotypes of strains employed in this study are listed in Table 1. The WT strains employed for these experiments were from the W303 background. Most deletion strains were created by either PCR amplifying the KanMX cassette from the homozygous diploid deletion collection (Research Genetics) or fusion PCR (63). Cells were grown in YPD (1% yeast extract, 2% peptone, 2% dextrose), YPGE (2% glycerol/ethanol), CM (0.67% yeast nitrogen base, 0.12% drop-out amino acid mixture, 2% dextrose), CM with 2% galactose or 2% glycerol/ethanol. Media were made iron-deficient by the addition of 80 μM BPS, and specific concentrations of ferrous sulfate (μM) were added back. The concentration of added iron in μM is denoted as BPS(x). Plasmids used in this study are listed in Table 2. Strains with β-estradiol–regulated expression plasmids consist of a Gal4 fused to an estrogen-responsive VP16 activation domain expressed from the MRP7 promoter as described (20) and a plasmid with a GAL1 promoter driving expression of *ERG29* or *ERG25*. To induce *ERG25* or *ERG29* expression, cells were grown in 50 nM β-estradiol-containing (Sigma) or galactose-containing medium. APB was added to growth medium at various concentrations, or cobalt chloride ($CoCl_2$, 1.0 mM) was added to growth medium. Cells were grown for 2–4 days on plates and overnight in liquid medium.

Suppressor library screen

Δ*erg29* cells containing *pYCpERG29 URA3* were transformed with a high-copy YEp-*LEU2* genomic library. Colonies were selected on −uracil−leucine. Colonies were replicated onto 5-fluoroorotic acid to allow loss of the *URA3 ERG29* plasmid, and colonies were plated onto YPGE. Colonies positive for growth on YPGE were identified, genomic preparations were made, and rescued plasmids were sequenced and identified genes subcloned to determine the gene(s) responsible for suppression. To confirm suppression of the poor growth due to loss of *ERG29* Δ*erg29pGAL1ERG29* (*TRP1*), cells were transformed with p*YFH1*, p*MMT1*, p*MMT2*, or p*PET20* (*LEU2* plasmids), and growth on CM−trp−leu−his galactose or glucose was assessed.

Sterol analysis

Cells were grown in galactose-containing medium overnight, shifted to glucose-containing medium for 18 h, pelleted, washed, and frozen at −80 °C. Lipid extractions were per-

formed on frozen cell pellets as described (64). All GC/MS sterol analysis was performed with an Agilent 7200 gas chromatograph-mass spectrometer fit with an Agilent 7693A autosampler (Agilent Technologies, Santa Clara, CA). Dried samples were suspended in 40 μl of pyridine, followed by transfer to autosampler vials, and 80 μl of *N*-methyl-*N*-trimethylsilyltrifluoracetamide (Thermo Fisher) was added automatically via the autosampler and incubated for 30 min at 37 °C with shaking. After incubation, 1 μl of the prepared sample was injected into the gas chromatograph inlet in the split mode with the inlet temperature held at 250 °C. A 25:1 split ratio was used for analysis. The gas chromatograph had an initial temperature of 60 °C for 1 min followed by a 10 °C/min ramp to 325 °C and a hold time of 2 min. A 30-m Agilent Zorbax DB-5MS with a 10-m Duraguard capillary column was employed for chromatographic separation. Helium was used as the carrier gas at a rate of 1 ml/min. Data were collected using MassHunter software (Agilent). Metabolites were identified, and their peak area was recorded using MassHunter Quant. These data were transferred to an Excel spreadsheet (Microsoft Corp., Redmond, WA).

MitoSOX flow cytometry

Δ*erg29pGAL1ERG29* plus or minus suppressor-identified plasmids was grown in galactose-containing medium overnight, shifted to glucose-containing medium for 16–18 h, and incubated with 20 nM MitoSOX according to the manufacturer's instructions (Thermo Fisher), and fluorescence was detected using a BD FACSCanto running FACSDiva version 8.0 software.

Other procedures and reagents

Quantitative PCR primers for *YFH1*, *ISU1*, and *ACT1* were *YFH1* forward GTCCAGCTGTAACAAATAAAA and reverse GTGCAATTTCTTAACGAAACCC, *ISU1* forward CAAGA-AACGTCGGCTCATTA and reverse GTCCAAGGTCATC-CCCTGTA, and *ACT1* forward TGTCACCAACTGGG-ACGATA and reverse GGCTTGGGATGGAAACGTAGA. Differential interference contrast and epifluorescence images were captured using an Olympus BX51 microscope with a ×100, 1.3 numerical aperture oil immersion objective and Pictureframer software. Aconitase activity was determined as described previously (42). For mitochondrial isolations, cells were digested and homogenized, crude mitochondrial pellets were obtained by centrifugation at 10,000 × *g* for 10 min, mem-

branes were solubilized, and protein determinations were performed as described previously (65). Proteins were analyzed by 4–20% SDS-PAGE Tris/glycine followed by Western blot analysis using Western Lightning (PerkinElmer Life Sciences). Antisera used for probing Western blots included rabbit anti-His$_6$ (1:1000), rabbit anti-Erg25 (1:500), rabbit anti-Yfh1 (1:1000), rabbit anti-Nfs1 (1:1000), rabbit anti-Isu1 (1:1000), rabbit anti-Ssq1 (1:1000), or mouse anti-porin (1:1000). Secondary antibodies were either peroxidase-conjugated goat anti-rabbit IgG or peroxidase-conjugated goat anti-mouse IgG (Jackson ImmunoResearch Laboratories; 1:5000). Western blots were quantified using Bio-Rad ImageLab^{TM} software. Cells were made Rho^O by incubating them in the presence of ethidium bromide overnight. Statistical analyses were performed using a two-tailed Student's t test with significance set at $p = 0.05$ (*), 0.01 (**), 0.001 (***), and 0.0001 (****).

References

1. Braymer, J. J., and Lill, R. (2017) Iron-sulfur cluster biogenesis and trafficking in mitochondria. *J. Biol. Chem.* **292,** 12754–12763 CrossRef Medline
2. Lill, R., Hoffmann, B., Molik, S., Pierik, A. J., Rietzschel, N., Stehling, O., Uzarska, M. A., Webert, H., Wilbrecht, C., and Mühlenhoff, U. (2012) The role of mitochondria in cellular iron-sulfur protein biogenesis and iron metabolism. *Biochim. Biophys. Acta* **1823,** 1491–1508 CrossRef Medline
3. Aloria, K., Schilke, B., Andrew, A., and Craig, E. A. (2004) Iron-induced oligomerization of yeast frataxin homologue Yfh1 is dispensable *in vivo*. *EMBO Rep.* **5,** 1096–1101 CrossRef Medline
4. Babcock, M., de Silva, D., Oaks, R., Davis-Kaplan, S., Jiralerspong, S., Montermini, L., Pandolfo, M., and Kaplan, J. (1997) Regulation of mitochondrial iron accumulation by Yfh1p, a putative homolog of frataxin. *Science* **276,** 1709–1712 CrossRef Medline
5. Chen, O. S., Hemenway, S., and Kaplan, J. (2002) Inhibition of Fe-S cluster biosynthesis decreases mitochondrial iron-export: evidence that Yfh1p affects Fe-S cluster synthesis. *Proc. Natl. Acad. Sci. U.S.A.* **99,** 16922–16927 CrossRef Medline
6. Chen, O. S., and Kaplan, J. (2001) YFH1-mediated iron homeostasis is independent of mitochondrial respiration. *FEBS Lett.* **509,** 131–134 CrossRef Medline
7. Lesuisse, E., Santos, R., Matzanke, B. F., Knight, S. A., Camadro, J. M., and Dancis, A. (2003) Iron use for haeme synthesis is under control of the yeast frataxin homologue (Yfh1). *Hum. Mol. Genet.* **12,** 879–889 CrossRef Medline
8. Ranatunga, W., Gakh, O., Galeano, B. K., Smith, D. Y., 4th, Söderberg, C. A., Al-Karadaghi, S., Thompson, J. R., and Isaya, G. (2016) Architecture of the yeast mitochondrial iron-sulfur cluster assembly machinery: the sub-complex formed by the iron donor, Yfh1 protein, and the scaffold, Isu1 protein. *J. Biol. Chem.* **291,** 10378–10398 CrossRef Medline
9. Santos, R., Dancis, A., Eide, D., Camadro, J. M., and Lesuisse, E. (2003) Zinc suppresses the iron accumulation phenotype of *Saccharomyces cerevisiae* lacking the yeast frataxin homologue (Yfh1). *Biochem. J.* **375,** 247–254 CrossRef Medline
10. Seguin, A., Bayot, A., Dancis, A., Rogowska-Wrzesinska, A., Auchère, F., Camadro, J. M., Bulteau, A. L., and Lesuisse, E. (2009) Overexpression of the yeast frataxin homolog (Yfh1): contrasting effects on iron-sulfur cluster assembly, heme synthesis and resistance to oxidative stress. *Mitochondrion* **9,** 130–138 CrossRef Medline
11. Seguin, A., Santos, R., Pain, D., Dancis, A., Camadro, J. M., and Lesuisse, E. (2011) Co-precipitation of phosphate and iron limits mitochondrial phosphate availability in *Saccharomyces cerevisiae* lacking the yeast frataxin homologue (YFH1). *J. Biol. Chem.* **286,** 6071–6079 CrossRef Medline
12. Cook, J. D., Bencze, K. Z., Jankovic, A. D., Crater, A. K., Busch, C. N., Bradley, P. B., Stemmler, A. J., Spaller, M. R., and Stemmler, T. L. (2006) Monomeric yeast frataxin is an iron-binding protein. *Biochemistry* **45,** 7767–7777 CrossRef Medline
13. Cook, J. D., Kondapalli, K. C., Rawat, S., Childs, W. C., Murugesan, Y., Dancis, A., and Stemmler, T. L. (2010) Molecular details of the yeast frataxin-Isu1 interaction during mitochondrial Fe-S cluster assembly. *Biochemistry* **49,** 8756–8765 CrossRef Medline
14. Moretti-Almeida, G., Netto, L. E., and Monteiro, G. (2013) The essential gene YMR134W from *Saccharomyces cerevisiae* is important for appropriate mitochondrial iron utilization and the ergosterol biosynthetic pathway. *FEBS Lett.* **587,** 3008–3013 CrossRef Medline
15. Polevoda, B., Panciera, Y., Brown, S. P., Wei, J., and Sherman, F. (2006) Phenotypes of yeast mutants lacking the mitochondrial protein Pet20p. *Yeast* **23,** 127–139 CrossRef Medline
16. Bard, M., Bruner, D. A., Pierson, C. A., Lees, N. D., Biermann, B., Frye, L., Koegel, C., and Barbuch, R. (1996) Cloning and characterization of ERG25, the *Saccharomyces cerevisiae* gene encoding C-4 sterol methyl oxidase. *Proc. Natl. Acad. Sci. U.S.A.* **93,** 186–190 CrossRef Medline
17. Gachotte, D., Pierson, C. A., Lees, N. D., Barbuch, R., Koegel, C., and Bard, M. (1997) A yeast sterol auxotroph (erg25) is rescued by addition of azole antifungals and reduced levels of heme. *Proc. Natl. Acad. Sci. U.S.A.* **94,** 11173–11178 CrossRef Medline
18. Li, L., and Kaplan, J. (1996) Characterization of yeast methyl sterol oxidase (ERG25) and identification of a human homologue. *J. Biol. Chem.* **271,** 16927–16933 CrossRef Medline
19. Snoek, I. S., and Steensma, H. Y. (2006) Why does *Kluyveromyces lactis* not grow under anaerobic conditions? Comparison of essential anaerobic genes of *Saccharomyces cerevisiae* with the *Kluyveromyces lactis* genome. *FEMS Yeast Res.* **6,** 393–403 CrossRef Medline
20. Gao, C. Y., and Pinkham, J. L. (2000) Tightly regulated, β-estradiol dose-dependent expression system for yeast. *BioTechniques* **29,** 1226–1231 Medline
21. Gachotte, D., Barbuch, R., Gaylor, J., Nickel, E., and Bard, M. (1998) Characterization of the *Saccharomyces cerevisiae* ERG26 gene encoding the C-3 sterol dehydrogenase (C-4 decarboxylase) involved in sterol biosynthesis. *Proc. Natl. Acad. Sci. U.S.A.* **95,** 13794–13799 CrossRef Medline
22. Huh, W. K., Falvo, J. V., Gerke, L. C., Carroll, A. S., Howson, R. W., Weissman, J. S., and O'Shea, E. K. (2003) Global analysis of protein localization in budding yeast. *Nature* **425,** 686–691 CrossRef Medline
23. Lee, H., Bien, C. M., Hughes, A. L., Espenshade, P. J., Kwon-Chung, K. J., and Chang, Y. C. (2007) Cobalt chloride, a hypoxia-mimicking agent, targets sterol synthesis in the pathogenic fungus *Cryptococcus neoformans*. *Mol Microbiol.* **65,** 1018–1033 CrossRef Medline
24. Paulsen, I. T., and Saier, M. H., Jr. (1997) A novel family of ubiquitous heavy metal ion transport proteins. *J. Membr. Biol.* **156,** 99–103 CrossRef Medline
25. Li, L., Miao, R., Jia, X., Ward, D. M., and Kaplan, J. (2014) Expression of the yeast cation diffusion facilitators Mmt1 and Mmt2 affects mitochondrial and cellular iron homeostasis: evidence for mitochondrial iron export. *J. Biol. Chem.* **289,** 17132–17141 CrossRef Medline
26. Foury, F., and Roganti, T. (2002) Deletion of the mitochondrial carrier genes MRS3 and MRS4 suppresses mitochondrial iron accumulation in a yeast frataxin-deficient strain. *J. Biol. Chem.* **277,** 24475–24483 CrossRef Medline
27. Mühlenhoff, U., Stadler, J. A., Richhardt, N., Seubert, A., Eickhorst, T., Schweyen, R. J., Lill, R., and Wiesenberger, G. (2003) A specific role of the

yeast mitochondrial carriers MRS3/4p in mitochondrial iron acquisition under iron-limiting conditions. *J. Biol. Chem.* **278,** 40612–40620 CrossRef Medline

28. Zhang, Y., Lyver, E. R., Knight, S. A., Lesuisse, E., and Dancis, A. (2005) Frataxin and mitochondrial carrier proteins, Mrs3p and Mrs4p, cooperate in providing iron for heme synthesis. *J. Biol. Chem.* **280,** 19794–19807 CrossRef Medline

29. Zhang, Y., Lyver, E. R., Knight, S. A., Pain, D., Lesuisse, E., and Dancis, A. (2006) Mrs3p, Mrs4p, and frataxin provide iron for Fe-S cluster synthesis in mitochondria. *J. Biol. Chem.* **281,** 22493–22502 CrossRef Medline

30. Mühlenhoff, U., Richhardt, N., Gerber, J., and Lill, R. (2002) Characterization of iron-sulfur protein assembly in isolated mitochondria: a requirement for ATP, NADH, and reduced iron. *J. Biol. Chem.* **277,** 29810–29816 CrossRef Medline

31. Radisky, D. C., Babcock, M. C., and Kaplan, J. (1999) The yeast frataxin homologue mediates mitochondrial iron efflux: evidence for a mitochondrial iron cycle. *J. Biol. Chem.* **274,** 4497–4499 CrossRef Medline

32. Hiltunen, J. K., Autio, K. J., Schonauer, M. S., Kursu, V. A., Dieckmann, C. L., and Kastaniotis, A. J. (2010) Mitochondrial fatty acid synthesis and respiration. *Biochim. Biophys. Acta* **1797,** 1195–1202 CrossRef Medline

33. Lill, R., and Mühlenhoff, U. (2005) Iron-sulfur-protein biogenesis in eukaryotes. *Trends Biochem. Sci.* **30,** 133–141 CrossRef Medline

34. Schonauer, M. S., Kastaniotis, A. J., Kursu, V. A., Hiltunen, J. K., and Dieckmann, C. L. (2009) Lipoic acid synthesis and attachment in yeast mitochondria. *J. Biol. Chem.* **284,** 23234–23242 CrossRef Medline

35. Melber, A., Na, U., Vashisht, A., Weiler, B. D., Lill, R., Wohlschlegel, J. A., and Winge, D. R. (2016) Role of Nfu1 and Bol3 in iron-sulfur cluster transfer to mitochondrial clients. *Elife* **5,** e15991 CrossRef Medline

36. Navarro-Sastre, A., Tort, F., Stehling, O., Uzarska, M. A., Arranz, J. A., Del Toro, M., Labayru, M. T., Landa, J., Font, A., Garcia-Villoria, J., Merinero, B., Ugarte, M., Gutierrez-Solana, L. G., Campistol, J., Garcia-Cazorla, A., *et al.* (2011) A fatal mitochondrial disease is associated with defective NFU1 function in the maturation of a subset of mitochondrial Fe-S proteins. *Am. J. Hum. Genet.* **89,** 656–667 CrossRef Medline

37. Mühlenhoff, U., Balk, J., Richhardt, N., Kaiser, J. T., Sipos, K., Kispal, G., and Lill, R. (2004) Functional characterization of the eukaryotic cysteine desulfurase Nfs1p from *Saccharomyces cerevisiae. J. Biol. Chem.* **279,** 36906–36915 CrossRef Medline

38. Li, J., Kogan, M., Knight, S. A., Pain, D., and Dancis, A. (1999) Yeast mitochondrial protein, Nfs1p, coordinately regulates iron-sulfur cluster proteins, cellular iron uptake, and iron distribution. *J. Biol. Chem.* **274,** 33025–33034 CrossRef Medline

39. Mühlenhoff, U., Gerber, J., Richhardt, N., and Lill, R. (2003) Components involved in assembly and dislocation of iron-sulfur clusters on the scaffold protein Isu1p. *EMBO J.* **22,** 4815–4825 CrossRef Medline

40. Lutz, T., Westermann, B., Neupert, W., and Herrmann, J. M. (2001) The mitochondrial proteins Ssq1 and Jac1 are required for the assembly of iron sulfur clusters in mitochondria. *J. Mol. Biol.* **307,** 815–825 CrossRef Medline

41. Voisine, C., Schilke, B., Ohlson, M., Beinert, H., Marszalek, J., and Craig, E. A. (2000) Role of the mitochondrial Hsp70s, Ssc1 and Ssq1, in the maturation of Yfh1. *Mol. Cell. Biol.* **20,** 3677–3684 CrossRef Medline

42. Li, L., and Kaplan, J. (2004) A mitochondrial-vacuolar signaling pathway in yeast that affects iron and copper metabolism. *J. Biol. Chem.* **279,** 33653–33661 CrossRef Medline

43. Lin, H., Li, L., Jia, X., Ward, D. M., and Kaplan, J. (2011) Genetic and biochemical analysis of high iron toxicity in yeast: iron toxicity is due to the accumulation of cytosolic iron and occurs under both aerobic and anaerobic conditions. *J. Biol. Chem.* **286,** 3851–3862 CrossRef Medline

44. Foury, F., and Cazzalini, O. (1997) Deletion of the yeast homologue of the human gene associated with Friedreich's ataxia elicits iron accumulation in mitochondria. *FEBS Lett.* **411,** 373–377 CrossRef Medline

45. Hoepfner, D., Helliwell, S. B., Sadlish, H., Schuierer, S., Filipuzzi, I., Brachat, S., Bhullar, B., Plikat, U., Abraham, Y., Altorfer, M., Aust, T., Baeriswyl, L., Cerino, R., Chang, L., Estoppey, D., *et al.* (2014) High-resolution chemical dissection of a model eukaryote reveals targets, pathways and gene functions. *Microbiol. Res.* **169,** 107–120 CrossRef Medline

46. Lee, A. Y., St. Onge, R. P., Proctor, M. J., Wallace, I. M., Nile, A. H., Spagnuolo, P. A., Jitkova, Y., Gronda, M., Wu, Y., Kim, M. K., Cheung-Ong, K., Torres, N. P., Spear, E. D., Han, M. K., Schlecht, U., *et al.* (2014) Mapping the cellular response to small molecules using chemogenomic fitness signatures. *Science* **344,** 208–211 CrossRef Medline

47. Ness, F., Bourot, S., Régnacq, M., Spagnoli, R., Bergès, T., and Karst, F. (2001) SUT1 is a putative Zn[II]2Cys6-transcription factor whose upregulation enhances both sterol uptake and synthesis in aerobically growing *Saccharomyces cerevisiae* cells. *Eur. J. Biochem.* **268,** 1585–1595 CrossRef Medline

48. Alimardani, P., Régnacq, M., Moreau-Vauzelle, C., Ferreira, T., Rossignol, T., Blondin, B., and Bergès, T. (2004) SUT1-promoted sterol uptake involves the ABC transporter Aus1 and the mannoprotein Dan1 whose synergistic action is sufficient for this process. *Biochem. J.* **381,** 195–202 CrossRef Medline

49. Baudry, K., Swain, E., Rahier, A., Germann, M., Batta, A., Rondet, S., Mandala, S., Henry, K., Tint, G. S., Edlind, T., Kurtz, M., and Nickels, J. T., Jr. (2001) The effect of the erg26-1 mutation on the regulation of lipid metabolism in *Saccharomyces cerevisiae. J. Biol. Chem.* **276,** 12702–12711 CrossRef Medline

50. Söderberg, C. A., Rajan, S., Shkumatov, A. V., Gakh, O., Schaefer, S., Ahlgren, E. C., Svergun, D. I., Isaya, G., and Al-Karadaghi, S. (2013) The molecular basis of iron-induced oligomerization of frataxin and the role of the ferroxidation reaction in oligomerization. *J. Biol. Chem.* **288,** 8156–8167 CrossRef Medline

51. Chen, O. S., Crisp, R. J., Valachovic, M., Bard, M., Winge, D. R., and Kaplan, J. (2004) Transcription of the yeast iron regulon responds not directly to iron but rather to iron-sulfur cluster biosynthesis. *J. Biol. Chem.* **279,** 29513–29518 CrossRef Medline

52. Akins, R. A. (2005) An update on antifungal targets and mechanisms of resistance in *Candida albicans. Med. Mycol.* **43,** 285–318 CrossRef Medline

53. Demuyser, L., Swinnen, E., Fiori, A., Herrera-Malaver, B., Vestrepen, K., and Van Dijck, P. (2017) Mitochondrial cochaperone Mge1 is involved in regulating susceptibility to fluconazole in *Saccharomyces cerevisiae* and *Candida* species. *MBio* **8,** e00201-17 Medline

54. Kalyanaraman, B. (2007) Iron signaling and oxidant damage. *Cardiovasc. Toxicol.* **7,** 92–94 CrossRef Medline

55. Kwok, J. C., and Richardson, D. R. (2004) Examination of the mechanism(s) involved in doxorubicin-mediated iron accumulation in ferritin: studies using metabolic inhibitors, protein synthesis inhibitors, and lysosomotropic agents. *Mol. Pharmacol.* **65,** 181–195 CrossRef Medline

56. Cocco, E., Porrini, V., Derosas, M., Nardi, V., Biasiotto, G., Maccarinelli, F., and Zanella, I. (2013) Protective effect of mitochondrial ferritin on cytosolic iron dysregulation induced by doxorubicin in HeLa cells. *Mol. Biol. Rep.* **40,** 6757–6764 CrossRef Medline

57. Maccarinelli, F., Gammella, E., Asperti, M., Regoni, M., Biasiotto, G., Turco, E., Altruda, F., Lonardi, S., Cornaghi, L., Donetti, E., Recalcati, S., Poli, M., Finazzi, D., Arosio, P., and Cairo, G. (2014) Mice lacking mitochondrial ferritin are more sensitive to doxorubicin-mediated cardiotoxicity. *J. Mol. Med.* **92,** 859–869 CrossRef Medline

58. Ichikawa, Y., Bayeva, M., Ghanefar, M., Potini, V., Sun, L., Mutharasan, R. K., Wu, R., Khechaduri, A., Jairaj Naik, T., and Ardehali, H. (2012) Disruption of ATP-binding cassette B8 in mice leads to cardiomyopathy through a decrease in mitochondrial iron export. *Proc. Natl. Acad. Sci. U.S.A.* **109,** 4152–4157 CrossRef Medline

59. Mouli, S., Nanayakkara, G., AlAlasmari, A., Eldoumani, H., Fu, X., Berlin, A., Lohani, M., Nie, B., Arnold, R. D., Kavazis, A., Smith, F., Beyers, R., Denney, T., Dhanasekaran, M., Zhong, J., *et al.* (2015) The role of frataxin in doxorubicin-mediated cardiac hypertrophy. *Am. J. Physiol. Heart Circ. Physiol.* **309,** H844–H859 CrossRef Medline

60. Runko, A. P., Griswold, A. J., and Min, K. T. (2008) Overexpression of frataxin in the mitochondria increases resistance to oxidative stress and extends lifespan in *Drosophila. FEBS Lett.* **582,** 715–719 CrossRef Medline

61. Kim, M. J., Kim, D. W., Yoo, K. Y., Sohn, E. J., Jeong, H. J., Kang, H. W., Shin, M. J., Ahn, E. H., An, J. J., Kwon, S. W., Kim, Y. N., Won, M. H., Cho,

ASBMB

S. W., Park, J., Eum, W. S., and Choi, S. Y. (2010) Protective effects of transduced PEP-1-Frataxin protein on oxidative stress-induced neuronal cell death. *J. Neurol. Sci.* **298,** 64–69 CrossRef Medline

62. Kim, M. J., Kim, D. W., Jeong, H. J., Sohn, E. J., Shin, M. J., Ahn, E. H., Kwon, S. W., Kim, Y. N., Kim, D. S., Park, J., Eum, W. S., Hwang, H. S., and Choi, S. Y. (2012) Tat-Frataxin protects dopaminergic neuronal cells against MPTP-induced toxicity in a mouse model of Parkinson's disease. *Biochimie* **94,** 2448–2456 CrossRef Medline

63. Amberg, D. C., Botstein, D., and Beasley, E. M. (1995) Precise gene disruption in *Saccharomyces cerevisiae* by double fusion polymerase chain reaction. *Yeast* **11,** 1275–1280 CrossRef Medline

64. Arthington-Skaggs, B. A., Jradi, H., Desai, T., and Morrison, C. J. (1999) Quantitation of ergosterol content: novel method for determination of fluconazole susceptibility of *Candida albicans. J. Clin. Microbiol.* **37,** 3332–3337 Medline

65. Li, L., Chen, O. S., McVey Ward, D., and Kaplan, J. (2001) CCC1 is a transporter that mediates vacuolar iron storage in yeast. *J. Biol. Chem.* **276,** 29515–29519 CrossRef Medline

66. Li, L., and Kaplan, J. (1997) Characterization of two homologous yeast genes that encode mitochondrial iron transporters. *J. Biol. Chem.* **272,** 28485–28493 CrossRef Medline

67. Li, F. Y., Nikali, K., Gregan, J., Leibiger, I., Leibiger, B., Schweyen, R., Larsson, C., and Suomalainen, A. (2001) Characterization of a novel human putative mitochondrial transporter homologous to the yeast mitochondrial RNA splicing proteins 3 and 4. *FEBS Lett.* **494,** 79–84 CrossRef Medline

68. Li, L., Miao, R., Bertram, S., Jia, X., Ward, D. M., and Kaplan, J. (2012) A role for iron-sulfur clusters in the regulation of transcription factor Yap5-dependent high iron transcriptional responses in yeast. *J. Biol. Chem.* **287,** 35709–35721 CrossRef Medline

ASBMB

J. Biol. Chem. (2018) 293(27) 10782–10795 **10795**